U. of Iowa 66-24

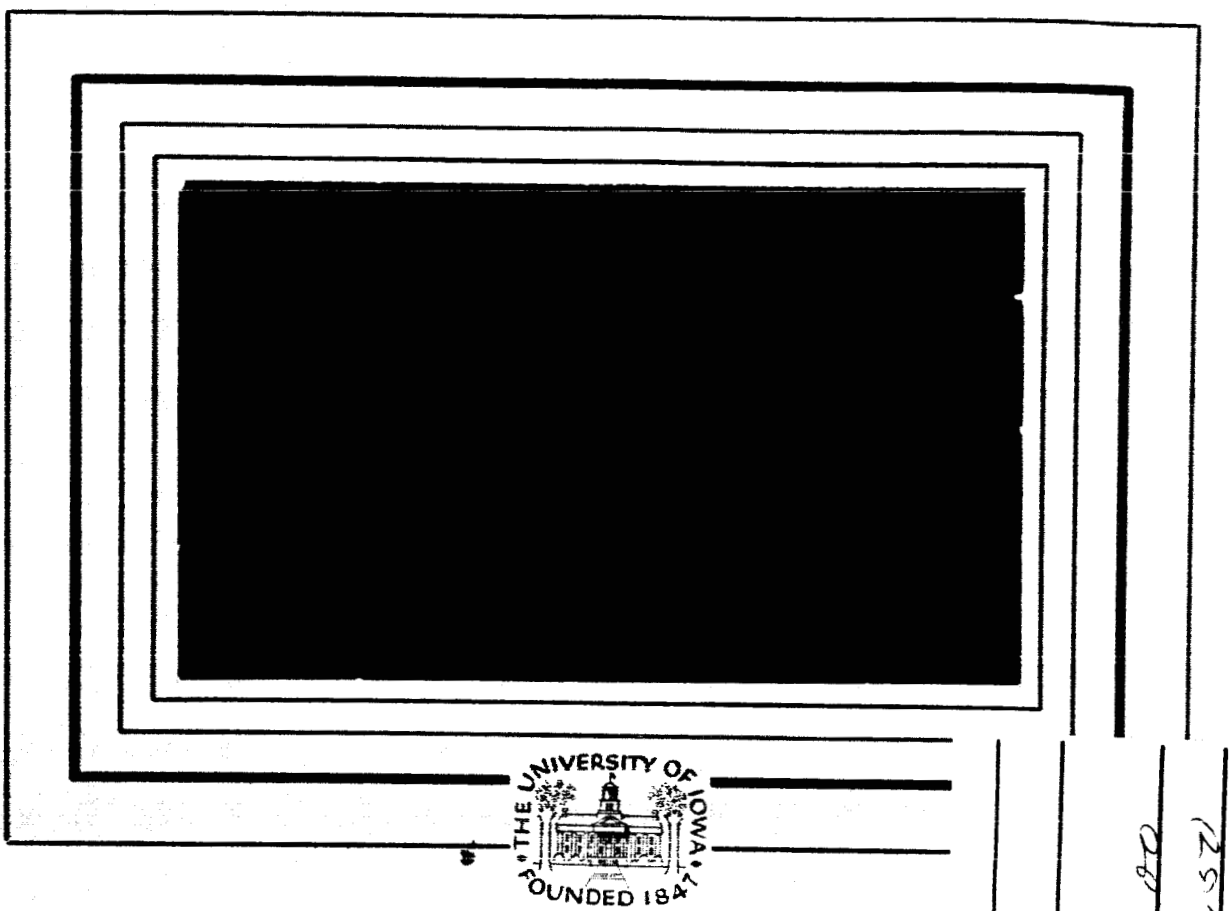

FACILITY FORM 602
N66 37517 (ACCESSION NUMBER)
52 (PAGES)
CR-78394 (NASA CR OR TMX OR AD NUMBER)
(THRU) 1
(CODE) 29
(CATEGORY)
GPO PRICE $
CFSTI PRICE(S) $
Hard copy (HC) 3.00
Microfiche (MF) .50
ff 653 July 65

Department of Physics and Astronomy
THE UNIVERSITY OF IOWA
Iowa City, Iowa

U. of Iowa 66-24

The Adiabatic Motion of Outer Zone Particles in a Model of the Geoelectric and Geomagnetic Fields *

by

Harold E. Taylor

Department of Physics and Astronomy
University of Iowa
Iowa City, Iowa

June 1966

*This work was supported in part by the National Aeronautics and Space Administration under research grant NsG-233-62.

ABSTRACT

Calculations of charged particle motions are carried out in a model of the earth's magnetosphere which includes both a magnetic field and an electric field. The magnetic field is an analytical approximation of the real field, based on extensive satellite measurements, while the electric field is deduced in the ionosphere from ionospheric current system and mapped throughout the magnetosphere by assuming that the magnetic field lines are equipotentials. Using this model the motions of charged particles are calculated by assuming that the first two adiabatic invariants, μ and J, and the total energy K are all conserved. Particle fluxes are then calculated by invoking Liouville's theorem.

The computations are done numerically on the University of Iowa, IBM 7044 computer and the results obtained for outer zone electrons are found to be in agreement with experimental measurements of the Injun 3 satellite.

Predictions of as yet unmeasured quantities are presented for comparison with future experiments.

I. INTRODUCTION

Many geophysical phenomena such as auroras, magnetic storms, and the radiation belts can be more satisfactorily understood if it is known how charged particles move in the electric and magnetic fields which constitute the magnetosphere. The determination of this motion involves two distinct parts: (1) the magnetospheric fields must be determined, and (2) the motion of the magnetospheric particles calculated.

The geomagnetic field has now been measured extensively by Explorers 10, 12, 14, and 18 and is relatively well known [Heppner et al., 1963; Cahill and Amazeen, 1963; Freeman et al., 1963; Freeman, 1964; Cahill, 1964; Ness et al., 1964; Ness, 1965]. It is confined by the solar wind to a cavity with a well defined boundary on the sunward side and is drawn out into a magnetic tail on the anti sunward side. In the tail Explorer 18 (Imp 1) discovered a thin neutral sheet near its center in which the magnetic field undergoes a sharp reversal of direction. The distortion of the magnetic field caused by this current sheet has important effects on the motion of charged particles.

Theoretical calculations of the effect of the solar wind on the earth's magnetic field have been presented by many authors [Spreiter and Briggs, 1962; Midgley and Davis, 1963; Mead and Beard, 1964; Mead, 1964; Axford et al., 1964]. These calculations are in general agreement both with each other and with experimental measurements. They provide a suitable basis for extrapolating the measurements to regions of the magnetosphere not yet traversed by satellites.

The magnetospheric electric field is not well known. It has not been directly measured, and indeed its direct measurement presents difficult experimental problems. The electric field used in this model was deduced from the ionospheric current system which, in turn, were deduced from magnetic disturbances observed at the earth (specifically from magnetic bay activity). There are many difficulties with this technique, although there do not appear to be any suitable alternatives.

A primary difficulty is the uncertainty in the current system itself. It has not been determined unequivocally, even in a long time average, and is quite variable from day to day and hour to hour. A second difficulty arises from the uncertainties which exist in the numerical values of the ionospheric conductivities.

Although they are fairly well known for low latitudes and normal conditions, they are expected to be quite different in the auroral zone where abnormally high ionization can be caused by the bombardment of auroral particles. Because the influx of these energetic particles is known to vary greatly in time, both the temperature and electron density are expected to be highly variable. This implies that the ionospheric conductivies will also be highly variable in the auroral zone. In fact it seems reasonable to speculate that these conductivity changes rather than changes in the electric field produce the large temporal variations observed in the currents.

A final uncertainty in the magnetospheric electric field is the assumption that the component of $\vec{E}$ parallel to the magnetic field lines, $E_{\parallel}$, is negligible compared to the component perpendicular to them. It has been shown by Bernstein et al. [1957] that equilibrium plasma distributions in which $E_{\parallel}$ is not zero can exist. The stability of these distributions has not been demonstrated, and they have not been observed in laboratory plasmas. In this work the assumption that $E_{\parallel} = 0$ is made without further justification.

The model fields which Dr. Hones and this author worked out are reported in an earlier paper [Taylor and Hones, 1965]. They incorporate the known features of the magnetic field and the "best"

assumption for the electric fields. Using this model of the magnetosphere, it is possible to calculate the motion of charged particles.

To carry out such calculations and to attempt to explain experimental measurements of the radiation belts, it is convenient to assume that the particle motion is adiabatic. This assumption appears to be reasonable for particles with energies between ~ 1 and 500 keV throughout the magnetosphere except on field lines which come within a few gyro radii of the magnetospheric surface and on field lines which penetrate the neutral sheet in the magnetospheric tail in regions where the thickness of this sheet is not several orders of magnitude greater than the particle gyro radius. In the radiation belts the field lines are smooth enough for adibatic theory to be valid.

Investigations similar to this one have been carried out previously [Hones, 1963; Maeda, 1964; Williams and Mead, 1965] but all are deficient in one or more of the important ingredients of the model used in this work. The calculations by Hones and those by Williams and Mead did not include an electric field. If the electric field is neglected, all particles having a given set of adiabatic invariants will follow the same paths regardless

of their energy. Thus, it is impossible to reproduce the energy dependent features of the radiation belts without a geoelectric field. The calculation by Maeda included an electric field but the applicability of his results to the real magnetosphere is limited by the fact that he used an undistorted dipole field and used only the low latitude, quiet day ionospheric current systems to obtain the electric field.

The uniqueness of the model used in this work is that it includes both the electric field which drives the high latitude (auroral zone) currents and a distorted magnetic field. In addition to the distortion caused by the solar wind impinging on the sunward boundary of the magnetosphere, the model magnetic field includes a current sheet in the magnetospheric tail. The effects of the non-alignment of the magnetic dipole axis and the rotational axis have been neglected as have the deviations of the earth's field from a dipole field near the earth. The calculation of particle motions is carried out under the assumption that the total energy and the first two adiabatic invariants are conserved.

II. CALCULATIONS OF PARTICLE FLUXES

In order to calculate particle fluxes it is convenient to calculate the trajectories of individual particles and then to invoke Liouville's theorem to calculate the variation of fluxes along these trajectories. The model magnetosphere presented by Taylor and Hones [1965] was used to calculate the trajectories. (The current sheet field was reduced to 20 γ and the electric field was slightly modified in the present calculation. See Taylor [1966] for details.) Figures 1 and 2 show the model fields used.

The adiabatic theory used to calculate the individual particle paths was also described in the earlier paper [Taylor and Hones, 1965]. The procedure followed was to calculate surfaces of constant longitudinal invariant, J, for particles having specified values of the total energy, K and the magnetic moment μ. This gave the motion of individual trapped particles.

The relationship between these individual particle paths and particle fluxes was determined by the use of a Liouville theorem. Northrop and Teller [1960] show that if Q is the number density of particles on a given field line with given values of μ and J, then Q obeys such a theorem. In a steady state situation then, Q is constant on a longitudinal invariant surface. It can easily be

shown that the number density of particles having specified μ and K is given by

$$n\ (\vec{r},\ K,\ \mu)\ d^3r\ dK\ d\mu = \frac{2B}{v_{\shortparallel}}\ Q\ d^3r\ dK\ d\mu\ .$$

(See Northrop and Teller [1960].) Here $\vec{r}$ is the position of the point in space, and $v_{\shortparallel}$ is the component of velocity parallel to $\vec{B}$. Now the flux of particles of the specified K and μ per unit K, per unit μ at position $\vec{r}$ is given by:

$$j = nv.$$

Thus

$$j\ (\vec{r},\ K,\ \mu) = 2B\ \frac{v}{v_{\shortparallel}}\ Q\ .$$

In terms of the pitch angle α, the flux of particles per unit K, per unit α at $\vec{r}$ is

$$j\ (\vec{r},\ K,\ \alpha) = 4\ WQ\ \sin\alpha,$$

or as is measured by differential satellite detectors the flux of particles per unit energy, per unit solid angle at $\vec{r}$ is

$$j\ (\vec{r},\ K,\ \Omega) = \frac{2WQ}{\pi}\ .$$

Now if the energy spectrum of the particles is exponential, then

$$Q \propto e^{-K/K_o} .$$

(Q is clearly invariant on a longitudinal invariant surface since K is invariant.) Then,

$$j(\vec{r}, W, \Omega) \propto W e^{-(W+qV)/K_o} .$$

The constant of proportionality is in general a function of the other invariants and gives the distribution of particle flux with J and μ.

A detector which samples a fixed energy, W, (or a fixed range of energies) will be sampling particles with a wide range of values of the invariants as it is moved from point to point in the magnetosphere. Thus, in order to calculate the particle fluxes, it is necessary that the distribution of particles with J and μ be known. In general the experimental results cannot give all the necessary information and further assumptions about the total distribution of particles in J and μ space must be made.

If it can be assumed that the particle distribution is independent of μ (at least over the range of μ's to which a

given detector responds) then the necessary distribution is obtained by measuring the variation of particle intensity with latitude at a given longitude. This is the assumption used in this work for comparison with Injun 3 data. This assumption is reasonable because Injun 3 sampled a relatively small range of μ's with its trapped particle detectors. Having made this assumption, it is useful to write the expression for the flux of particles measured by a detector which responds to particles of a fixed energy.

$$j\ (r,\ \Omega) \propto e^{-qV/K_o} \quad .$$

(In obtaining this expression it has also been assumed that the particle energy spectrum is exponential with an e-folding energy of K_o.)

The flux at a given point in the magnetosphere was determined in the following manner. First the longitudinal invariant surface (surfaces) on which the detected particles are moving was determined from the position of the detector, the particle pitch angles, and energies. Then the flux desired is given by the flux on this invariant surface measured at a reference longitude multiplied by the factor $e^{-q(V-V_o)/K_o}$ where V_o is the potential of the invariant surface at the reference longitude. Although this procedure was tedious in practice, it is straightforward.

III. EXPERIMENTAL COMPARISONS

Numerous studies of particle intensities in the radiation zones and their variation with latitude, local time, and altitude have been carried out. The studies of particular interest in this work are the measurements of diurnal variations in outer zone electron intensities. O'Brien [1963] was the first to report a large diurnal variation in the high latitude boundary of trapped, $\gtrsim$ 40 keV electrons. Using the Injun 1 satellite, this boundary was found to be roughly six degrees higher in latitude at local noon than at local midnight (~ 75° at local noon; ~ 69° at local midnight). Similar results were obtained by McDiarmid and Burrows [1964] using detectors on the Alouette satellite. More complete studies of the variation of the intensity versus latitude profile for electrons $\gtrsim$ 40 keV were carried out using the Injun 3 satellite and were reported by Frank et al. [1964].

An indication of the dependence of the diurnal shifts in the outer zone on electron energy can be obtained from the work of Williams and Palmer [1965]. They reported the diurnal shifts of $\gtrsim$ 280 keV electrons to be ~ 3° between noon and midnight local time, again the particles being found at higher latitudes during the daytime. A more complete analysis of thin energy dependence was made by

Armstrong [1965] on an independent set of observations. He shows that the higher energy electrons ($W_e \gtrsim 230$ keV) have significantly smaller diurnal shifts than the lower energy ones, ($W_e \gtrsim 40$ keV). In this section we will be concerned with the comparison of predictions based on the model with observations made using detectors carried on the Injun 3 satellite. Specifically, we will be interested in two detectors measuring trapped electrons. One was sensitive to electrons with energies, $W_e \gtrsim 40$ keV and the second was sensitive to electrons with $W_e \gtrsim 230$ keV. These detectors had their acceptance cones oriented perpendicular to the magnetic field vector, so that they were sensitive to particles whose pitch angles were $90° \pm 13°$.

The satellite orbit was such that the magnetic field strength, B, varied at the satellite over the range $0.2 \lesssim B \lesssim 0.5$ gauss. Since the energy spectrum is known to be falling relatively rapidly with increasing energy, it is reasonable to assume that the low energy detector measured primarily electrons of ~ 50 keV while the higher energy detector measured particles of ~ 250 keV. The low energy detector was then measuring particles with μ in the range $100 < \mu < 250$ keV/gauss while the higher energy detector measured particles with $500 \lesssim \mu \lesssim 1250$ keV/gauss. This assumption concerning the energy of the particles creating the response of the detectors

is reasonable for an exponential energy spectrum of the form e^{-W/W_o} if $W_o \lesssim 25$ keV for the low energy detector and $W_o \lesssim 100$ keV for the higher energy detector. For a power law spectrum of the form $W^{-\gamma}$ we require $\gamma \gtrsim 3$ for both detectors. For spectra which do not fall in these categories, higher energy particles will contribute significantly to the detector responses, and more detailed calculations must be made to accurately determine the electron fluxes measured. The approximation used here should give a reasonable estimate of the detector response for the spectra encountered in the outer radiation zone.

The actual method used to predict the variations of particle fluxes with longitude was as follows. The aim was to predict the particle intensity, $j(\theta_o, \varphi_o)$, which the detector will measure on the field line specified by θ_o, φ_o. The first step was to determine appropriate values of the adiabatic invariants for the detected particles. For the low energy detector it was assumed that the energy of the detected particles was 45 keV and that the magnetic field strength at the satellite was 0.3 gauss. Then μ = 150 keV/gauss and $K(\theta_o, \varphi_o) = 45 - V(\theta_o, \varphi_o)$ keV. From the computer calculations for μ = 150 keV/gauss and the appropriate K, the longitudinal

invariant surface on which the particles moved, $J(\theta_o, \varphi_o, K, \mu)$, was determined. From this, the colatitude at which the detected particles must have crossed the noon meridian could be found. This colatitude will be written as $\theta_N(\theta_o, \varphi_o)$. Then an experimentally determined profile of intensity versus colatitude in the noon meridian plane, $j(\theta_N, 0)$, was introduced. The intensity observed by the detector on the specified field line is then given by

$$j(\theta_o, \varphi_o) = j(\theta_N, 0)\, e^{-q(V-V_o)/K_o}.$$

Here V_o is the potential of the field line emanating from a colatitude of θ_N in the noon meridian.

The method for the higher energy detector is identical except that the energy of the detected particles was assumed to be 250 keV. Then μ = 833 keV/gauss and $K(\theta_o, \varphi_o) = 250 - V(\theta_o, \varphi_o)$ keV.

The basic assumptions made in the above methods may be simply stated as follows:

1. The particle energy spectrum is exponential with an e-folding energy, K_o.

2. All the particles creating the detector response come from approximately the same colatitude at noon.

The first assumption was primarily for mathematical convenience. Experimenters commonly fit either an exponential curve (e^{-W/W_o}) or a power law curve ($W^{-\gamma}$) to their spectral measurements. Since these measurements usually consist of only a few points (typically three or four), both curves satisfactorily fit the data. In these calculations the mathematics would have been greatly complicated if a power law spectrum had been assumed.

The second assumption can be justified empirically on the basis of the individual particle trajectories previously calculated. For the low energy detector, the colatitude of K = 45 keV, μ = 150 keV/ gauss particles at noon are compared to the colatitudes of the other particles which contribute significantly to the detector response. For e-folding energies less than about 25 keV, the major contribution to the detector response comes from particles having energies between 40 and 55 keV. As mentioned earlier, the μ values range from ~ 100 keV/gauss to 250 keV/gauss. For such particles the maximum deviation of their position at noon from the position of the K = 45, μ = 150 particles were determined to be -0.8°, +1.3°. For most lines in the magnetosphere the deviation was much less. Thus, within about 1° of latitude the particles which produce the major part of the flux do come from the same field line at noon.

These results are summarized in Figures 3 and 4. Figure 4 shows the worst case of deviation and indicates that the assumption made is reasonable.

Similar analysis for the higher energy detector shows that the maximum deviation is less than 0.5° for electrons with energies between 230 and 280 keV and magnetic moments between 500 and 1000 keV/gauss. These deviations are so small that they cannot be clearly displayed in Figures like 3 and 4.

Because the variations of intensity with latitude in the noon meridian are not great (less than a factor of 2 per degree of latitude), the assumptions made should lead to reasonably accurate results. In addition, since the paths were calculated for an energy in the middle of the range of energies which make up the measured flux, much of the error for the low energy detector made by neglecting the path differences for electrons between 40 and 45 keV is offset by neglecting the path differences for electrons between 45 and 55 keV. A similar argument holds for the higher energy detector.

In light of the fact that the intensity of outer zone electrons is observed to undergo changes of an order of magnitude, the approximate results obtained using the method outlined above appear to be as accurate as warranted in this situation. More

accurate calculations would not be expected to give much better agreement with observations.

The experimental results with which the calculations are compared were obtained using the Injun 3 satellite. Comparison is first made with the results reported by Frank et al. [1964] and then with the more complete study by Armstrong [1965]. Frank et al. [1964] drew contours of constant intensity for trapped, $W_e \gtrsim 40$ keV electrons from intensities measured during the 9 months of operation of Injun 3. The profile of intensity versus latitude at noon was used for $j\ (\theta_N, 0)$, and the intensities at intervals of 30° in longitude was calculated at every degree of latitude. Then contours of constant intensity were drawn. The calculated points are shown together with the experimental curve in Figure 5.

The more complete study of Injun 3 data by Armstrong [1965] provides a more stringent test of the model. He determined profiles of median intensity of trapped electrons versus latitude using all available Injun 3 data. These profiles were determined separately in each of four different local time sectors for two different electron energy levels, $W_e \gtrsim 40$ keV and $W_e \gtrsim 230$ keV. If the intensity vs. latitude profile at noon is assumed to give $j\ (\theta_N, 0)$, and an e-folding energy, K_o, is assumed, the latitudinal profiles

of intensity can be calculated in the other longitudinal sectors. K_o was taken to be 20 keV for the $\gtrsim$ 40 keV electrons, and K_o = 100 keV was adopted for the $\gtrsim$ 230 keV electrons.

The intensity profiles were calculated every 30° in longitude giving three intensity predictions at each latitude in each of Armstrong's local time sectors. The median of these three values was taken to be the intensity for the whole sector at that latitude. The resulting points are plotted in Figures 6 and 7 against Armstrong's curves.

The error bars shown in the upper left-hand corner of each plot are the estimated average error introduced by all factors but become for practical purposes just the uncertainty in the experimental median intensities (~ factor of 1.5) for the vertical bars and an uncertainty of somewhat over .5° of latitude from the computational approximations for the horizontal bars.

Calculations were also carried out for $\gtrsim$ 40 keV electrons with e-folding energies of 10 keV and 40 keV but are qualitatively the same. For latitudes above ~ 65°, the calculations with K_o = 10 keV gave intensities which were roughly a factor of two higher while calculations with K_o = 40 keV gave intensities roughly one-half of those shown. The e-folding energy chosen for the $\gtrsim$ 230 keV electrons is not critical so long as it is $\gtrsim$ 70 keV.

The apparent disagreement between predicted points and observed curves at low latitudes is probably due to a hardening of the spectrum in this region. Such a hardening has been indicated by Fritz [1964] using Injun 3 data. If this is the case, more detailed calculations including a numerical integration of electron intensity over energy are required on each field line. Such detail was not felt to be warranted. One can say qualitatively that the intensities predicted at each longitude would not be greatly different from the intensity assumed at noon if the spectrum were significantly harder in this region.

VI. PREDICTIONS BASED ON THE MODEL

In the foregoing section, a comparison of calculations based on the model with experimental results was described with the aim of establishing the general validity of the model. In this section calculations of as yet unmeasured features of particle motions will be discussed. In particular, the section includes calculations of the motion of electrons with energies of 10 keV and less, motion of electrons in the equatorial plane, and the motion of trapped protons with energies less than about 500 keV. Scattered measurements of these quantities have been made, but extensive measurements of their spatial variations have not been made yet. Comparison of these calculated results with future experimental findings can thus be used to further determine the limits of the validity of the assumptions made in these calculations.

Unfortunately the model includes no specific mechanisms for generating the particles which are measured. Particle fluxes cannot be predicted unless it is known how the particles are distributed in K, μ, and J. Thus, the prediction of particle fluxes throughout the magnetosphere cannot be made until sufficient measurements have been made to determine the particle distribution. Because of this feature, predictions of unmeasured quantities must involve further assumptions.

If it were known how the fluxes of 10 keV electrons varied with latitude, altitude, and K at some longitude, it would be a simple matter to use the methods described in the previous section to calculate the fluxes at other longitudes. If it is assumed that only particles with $K > 0$ exist in the magnetosphere, the predictions shown in Figure 8 can be made for low mirroring 10 keV electrons. The heavily cross-hatched region at high latitudes is the region where particles from outside the magnetosphere may be found. These particles are not durably trapped, but after becoming trapped initially near the magnetospheric surface will drift in longitude around the magnetosphere once and be lost out through the magnetospheric surface again. Thus, in this region the presence of 10 keV particles will be highly dependent on conditions exterior to the magnetosphere.

It should be noted that there should be 10 keV electrons in at least the nighttime portion ($90° < \varphi_o < 270°$) of the heavily cross-hatched region even if there are no 10 keV electrons present in the source region outside the magnetosphere because the electric field will accelerate lower energy particles. This is roughly in agreement with the measurements of Fritz and Gurnett [1965]. They see electrons > 10 keV at high latitudes on the night side of the

magnetosphere with Injun 3 roughly where they are predicted to be by the model. Another feature of this region which should be pointed out is that its location is highly dependent on the configuration of the electric field. It should change as the electric potential system changes.

A final point which should be mentioned is that if there are large numbers of low energy ($\lesssim$ 1 keV) particles entering the magnetosphere near its surface, then they should be found along their drift paths with energies approximately equal to their charge times the potential difference between the point at which they are detected and the magnetospheric surface. Forthcoming measurements of electron fluxes for energies from $\lesssim$ 1 keV to $\sim$ 10 keV should see this behavior easily if it exists.

The lightly slashed region at lower latitudes is the region where durably trapped 10 keV electrons can be found mirroring at 0.3 gauss. (The region extends to latitudes below those shown in these diagrams.) The high latitude boundary of this lightly slashed region is limited on the night side by the restriction that K be greater than zero. On the day side the high latitude boundary is the highest latitude for which 10 keV particles mirroring at 0.3 gauss can drift completely around the earth without being energized so much

that they mirror in the atmosphere somewhere along their path. Thus, the boundary would not be sharp as indicated in the figure, but should be somewhat like the high latitude boundary of the energetic particles in the outer radiation zone. Because this boundary depends upon the energization of the electrons, it should change with changes in the electric field. However, because these electrons take a few hours to drift around the earth, the fluctuations in the boundary would not be expected to follow the variations in the electric field very faithfully. The contours of constant intensity within this region cannot be predicted in general without a knowledge of the intensity variations from some line across the region. However, since there is a definite loss mechanism acting to limit the poleward extent of this region, the contours of constant intensity near this northern boundary should be approximately parallel to the boundary.

The assumption $K > 0$ for particles in the magnetosphere is equivalent to assuming that the energetic particles must originate outside the magnetosphere, since they must have an energy greater than 0 at the magnetospheric surface where $V = 0$. Then at the surface $K = W > 0$ and the assumption that K is conserved implies that $K > 0$

throughout the magnetosphere. If particles could be accelerated from arbitrary points within the magnetosphere, then negative K's would be possible. Protons could have K's ranging down to the smallest potential which exists in the magnetosphere (i.e., largest negative potential) and electrons could have K's down to minus the largest positive potential. If the real fields vary sufficiently rapidly in time, then K will not be conserved and nothing can be said about allowed and forbidden values of K. Some of this uncertainty may also be resolved by forthcoming measurements of the energy spectrum of particles in the 1 to 10 keV range. If K is conserved, and particles cannot have $K > 0$, then in the region where the potentials are positive no electrons should be seen with an energy less than the potential of the point of the measurement. Similarly, in regions where the potentials are negative, no protons with energies less than minus the potential should be found. This picture will be complicated by the temporal variations which exist in the electric field; however, it should be possible to answer the questions posed above.

The motion of electrons in the equatorial plane is another quantity which can be conveniently calculated on the basis of the model. In this case, again a measurement of the fluxes as a function

of radial distances at one longitude and a measurement of the energy spectrum must be made before the intensities at other longitudes can be calculated. Figures 9 and 10 show contours of constant intensity for 50 keV electrons and 10 keV electrons, respectively. For the 50 keV electrons the intensity in the midnight meridian plane was taken from the report by Frank [1965]. The curves for the 10 keV electrons were calculated assuming the same variation of relative intensity with radial distance at midnight local time. The energy spectrum for both sets of particles was assumed to be exponential with an e-folding energy of 20 keV.

One point of interest here is that on the day side of the magnetosphere the minimum B value is not in the equatorial plane for many of the field lines. For field lines which cross the equatorial plane beyond ~ 9 R_E, there are two minima, one above the equatorial plane and the other below it. Thus, during the daytime the maximum intensities on a given field line are expected to be found near the neutral points rather than in the equatorial plane.

It is also interesting that on the field lines swept back over the polar cap by the solar wind, there is a local minimum near the neutral point. Thus, although these field lines extend far down the tail and cannot have particles bouncing back and

forth across the equatorial plane on them, they can have particles trapped near this minimum B region; and, thus, high inclination satellites with apogees greater than about 10 R_E may find a local maximum in the intensity near the neutral point even on field lines swept back into the magnetospheric tail. In this model the neutral points are at a radial distance of ~ 10 R_E and a magnetic latitude of ~ 55° in the noon meridian.

The last prediction to be discussed regards the motion of protons with energies $\lesssim$ 500 keV. Because the rigidity of protons is much greater than that of electrons having the same kinetic energy, protons found durably trapped in the outer radiation zone are expected to have much lower energies than the electrons trapped in the same region. A rough estimate of the maximum energy for stable trapping in the midnight meridian is shown in Figure 11. These curves were calculated by assuming that the particle gyro radius in the equatorial plane of the model was less than ρ_{Max} where ρ_{Max} was given by:

$$\rho_{Max} = \begin{cases} C & B_{cs} > B_{eq} \\ C\left(\frac{B_{eq}}{B_{cs}}\right) & B_{cs} \leq B_{eq} \end{cases}$$

Here B_{cs} is the field of the current sheet and B_{eq} is the equatorial field strength from the earth's dipole and its image. The constant, C, was determined empirically from measured cutoffs of trapped 40 keV electrons and is presumably related to the thickness of the current sheet. A value of 6 km was used.

These curves indicate that in the midnight meridian trapped protons should be seen only at relatively low latitudes. However, since the current sheet is primarily confined to the magnetospheric tail, the field lines on the sunward side of the earth will be relatively smooth. Kilovolt protons would be expected to be stably trapped except for field lines which come within a few gyro radii of the magnetospheric surface. Since the field lines on which these kilovolt protons are trapped are not significantly affected by the current sheet, the invariant surfaces for the higher energy particles will be approximately a constant L shell. The lower energy particles will be affected by the electric field. A consideration of the potential system in Figure 4 shows that such protons would be expected to be at their lowest latitudes in the afternoon. However, at these low latitudes, ($< 65°$), the electric field is relatively weak and would affect only the very low energy particles, ($\sim$ 1 keV). Thus on the basis of this model it is expected that

kilovolt protons will be found durably trapped only at $L \lesssim 5$ at all longitudes, and that in the steady state situation, when temporal variations are small, the diurnal variation of proton intensity should be small, $\sim 1^{\circ}$ of latitude.

VII. SUMMARY AND CONCLUSION

The goal of this study has been to carry out quantitative calculations of the motion of charged particles at high latitudes and to compare the results with experimentally measured quantities.

A quantitative comparison between measured and predicted electron fluxes in the outer radiation zone shows that these fluxes can be described by adiabatic theory if a distorted magnetic field and a magnetospheric electric field are included. The model used for the geomagnetic field includes the effects of the solar wind pressure on the sunward side of the earth and the effects of a neutral sheet forming an extended magnetic tail on the antisolar side. These features have been well, though incompletely mapped out by satellite-borne experiments. The geoelectric field has not been measured directly and in this work was deduced from ionospheric currents which have not been determined unequivocally themselves. In addition, the ionospheric conductivities which must be known in order to calculate the electric field are highly uncertain. In spite of the inaccuracy these uncertainties must introduce the motion of outer zone electrons calculated using the model fields and the adiabatic assumptions produces variation in the outer zone electron intensities which are in good agreement with the observed

variations. It is especially significant that the model correctly predicts the dependence of these variations on particle energy because it is only by including an electric field that an energy dependence can be created.

The agreement found between calculations and observations is taken to imply that the assumptions made in the calculations are reasonable. Specifically, the fact that the model correctly predicts the diurnal variations of energetic electrons ($W_e \gtrsim 230$ keV), whose paths are only slightly affected by the electric field, indicates that the model magnetic field is a reasonable representation of the real magnetic field. The fact that the model also correctly gives the much larger diurnal variations of lower energy electrons ($W_e \gtrsim 40$ keV) is evidence that the electric field used is a reasonable representation of the real magnetospheric electric field, at least in a long time (yearly) average. In addition the fact that the calculations agree for outer zone electrons indicates that the assumption of adiabatic motion is reasonable for these particles.

The picture presented here is admittedly a simplification of the real magnetosphere. Several known features of the real magnetosphere have not been included in the model because it was

felt that their inclusion would create complexity without introducing much, if any, physical insight. For example, the earth's internal field was assumed to be purely dipolar while in actuality it is known to contain higher order multipole terms. The inclusion of these terms as done by Mead [1964] and Williams and Mead [1965] should increase the accuracy of the calculations. The representation of the current sheet is highly simplified in these calculations; more accurate calculations might include the field of a specified, physical current distribution. Also the non-alignment of the geographic, geomagnetic, and solar ecliptic polar axis should be taken into account. However, because of the great variability and wide uncertainties in the magnetospheric phenomena of interest the inclusion of these details seems unwarranted. The main features of interest in the real magnetosphere should manifest themselves in this simplified model.

The great variability in the interesting features of the magnetosphere appears in itself to be an indication that there are many processes which are not understood at present which must eventually be included in a complete understanding of the magnetosphere. For instance, the particle source and its variations are almost completely unknown. The variations in the solar wind and

geomagnetic disturbances caused by them require much more study. The role of plasma instabilities in the magnetosphere is almost completely unknown although it would appear that they are almost certainly important in geomagnetic phenomena. It is encouraging that some magnetospheric phenomena can be understood in terms of a simplified model such as this, and it is hoped that such a model will grow to include new features of the magnetosphere as they become understood.

ACKNOWLEDGEMENTS

I would like to express my indebtedness to Dr. E. W. Hones, Jr., who initiated this study and provided much help throughout. I would also like to thank Professor James A. Van Allen and Dr. S.-I. Akasofu for their helpful suggestions and encouragement. I am grateful for the financial support of the National Aeronautics and Space Administration both through my predoctural fellowship and through their research grant, NsG-233-62.

REFERENCES

Armstrong, T., Morphology of the Outer Zone Electron Distribution at Low Altitudes from January through July and September 1963 from Injun 3, J. Geophys. Res., 70, 2077-2100, 1965.

Axford, W. I., H. E. Petschek, and G. L. Siscoe, The Tail of the Magnetosphere, Avco Everett Research Report No. 190, August 1964.

Bernstein, I. B., J. M. Greene, and M. D. Kruskal, Exact Nonlinear Plasma Oscillations, Phys. Rev., 108, 546-550, 1957.

Cahill, L. J., Jr., and P. G. Amazeen, The Boundary of the Geomagnetic Field, J. Geophys. Res., 68, 1835-1843, 1963.

Cahill, L. J., Jr., Preliminary Results of Magnetic-Field Measurements in the Tail of the Geomagnetic Cavity, I.G. Bulletin, 79, 1964.

Frank, L. A., J. A. Van Allen, and J. D. Craven, Large Diurnal Variations of Geomagnetically Trapped and of Precipitated Electrons Observed at Low Altitudes, J. Geophys. Res., 69, 3155-3167, 1964.

Frank, L. A., A Survey of Electrons > 40 keV Beyond 5 Earth Radii with Explorer 14, J. Geophys. Res., 70, 1593-1626, 1965.

Fritz, T. A., A Latitude Survey of the Electron Energy Spectrum in the Outer Zone, Unpublished masters dissertation, Department of Physics and Astronomy, University of Iowa, 1964.

Fritz, T. A., and D. A. Gurnett, Diurnal and Latitudinal Effects Observed for 10-Kev Electrons at Low Satellite Altitudes, J. Geophys. Res., 70, 2485-2502, 1965.

Freeman, J. W., J. A. Van Allen, and L. J. Cahill, Explorer 12 Observations of the Magnetospheric Boundary and the Associated Solar Plasma on September 13, 1961, J. Geophys. Res., 68, 2121-2130, 1963.

Freeman, J. W., Jr., The Morphology of the Electron Distribution in the Outer Radiation Zone and Near the Magnetospheric Boundary as Observed by Explorer 12, J. Geophys. Res., 69, 1691-1723, 1964.

Heppner, J. P., N. F. Ness, C. S. Scearce, and T. L. Skillman, Explorer 10 Magnetic Field Measurements, J. Geophys. Res., 68, 1-46, 1963.

Hones, E. W., Jr., Motion of Charged Particles Trapped in the Earth's Magnetosphere, J. Geophys. Res., 68, 1209-1219, 1963.

Maeda, H., Electric Fields in the Magnetosphere Associated with the Daily Geomagnetic Variations and Their Effects on Trapped Particles, J. Atm. Terr. Phys., 26, 1133-1138, 1964.

McDiarmid, I. B., and J. R. Burrows, High-latitude Boundary of the Outer Radiation Zone at 1000 km, Can. J. Phys., 42, 616-626, 1964.

Mead, G. D., and D. B. Beard, Shape of the Geomagnetic Field Solar Wind Boundary, J. Geophys. Res., 69, 1169-1179, 1964.

Mead, G. D., Deformation of the Geomagnetic Field by the Solar Wind, J. Geophys. Res., 69, 1181-1195, 1964.

Midgley, J. E., and L. Davis, Jr., Calculation by a Moment Technique of the Perturbation of the Geomagnetic Field by the Solar Wind, J. Geophys. Res., 68, 5111-5123, 1963.

Ness, N. F., C. S. Scearce, and J. B. Seek, Initial Results of the Imp 1 Magnetic Field Experiment, J. Geophys. Res., 69, 3531-3570, 1964.

Ness, N. F., The Earth's Magnetic Tail, J. Geophys. Res., 70, 2989-3005, 1965.

Northrop, T. G., and E. Teller, Stability of the Adiabatic Motion of Charged Particles in the Earth's Field, Phys. Rev., 117, 215-225, 1960.

O'Brien, B. J., A Large Diurnal Variation of the Geomagnetically Trapped Radiation, J. Geophys. Res., 68, 989-995, 1963.

Spreiter, J. R., and B. J. Briggs, Theoretical Determination of the Form of the Boundary of the Solar Corpuscular Steam Produced by Interaction with Magnetic Dipole Field of the Earth, J. Geophys. Res., 67, 37-51, 1962.

Taylor, H. E., and E. W. Hones, Jr., The Adibatic Motion of Auroral Particles in a Model of the Electric and Magnetic Fields Surrounding the Earth, J. Geophys. Res., 70, 3605-3628, 1965.

Taylor, H. E., The Adiabatic Motion of Charged Particles in a Model of the Geoelectric and Geomagnetic Fields, Unpublished Ph.D. Dissertation, Department of Physics and Astronomy, University of Iowa, February 1966.

Williams, D. J., and W. F. Palmer, Distortions in the Radiation Cavity as Measured by an 1100-Kilometer Polar Orbiting Satellite, J. Geophys. Res., 70, 557-567, 1965.

Williams, D. J., and G. D. Mead, A Nightside Magnetosphere Configuration as Obtained from Trapped Electrons at 1100 Kilometers, J. Geophys. Res., 70, 3017-3029, 1965.

FIGURE CAPTIONS

Figure 1. The model magnetic field and the coordinate system used. The X and Z axes are shown labeled in units of earth radii. The Y axis is out of the page. The earth's dipole moment and the image are shown. The field lines drawn are in the noon-midnight meridian plane and are labeled with their colatitude at the earth's surface.

Figure 2. Equipotentials of the electric field assumed. The zero of the potential system has been chosen to make the magnetospheric surface have zero potential. Curves are labeled in kilovolts. Latitude circles are labeled with colatitude in degrees. View is from above the north pole.

Figure 3. μ dependence of drift paths for individual electrons K = 40 keV.

Figure 4. Energy dependence of drift paths for low energy ($\sim$ 40 keV) electrons.

Figure 5. Comparison between experimental contours of constant intensity of trapped electrons, $W_e \gtrsim 40$ keV from Frank et al., [1964] and points of constant intensity predicted by model calculations. Experimental curves are labeled with median omnidirectional fluxes in (particles/cm^2 sec).

Figure 6. Comparison between experimental intensity vs. colatitude curves for trapped electrons, $W_e \gtrsim 40$ keV, from Armstrong [1965] and points predicted by model calculations. Armstrong's curve from the noon longitudinal sector is used to predict the fluxes in the other three longitudinal sectors. The results from all four sectors are compared in the lower right.

Figure 7. Same as Figure 35 for $W_e \gtrsim 230$ keV.

Figure 8. Regions where, on the basis of the model, 10 keV electrons are expected to be found mirroring at 0.3 gauss. The cross hatched region is where the electrons from outside the magnetosphere will be found. The slashed region is where durably trapped 10 keV electrons can be found.

Figure 9. Contours of constant directional intensity of 50 keV electrons in the equatorial plane calculated on the basis of the model. The distribution of intensity with radial distance at midnight was taken from Frank [1965]. Curves are labeled in (particles/cm^2 sec sterad).

Figure 10. Similar to Figure 9 for 10 keV electrons. The distribution of intensity with radial distance assumed at midnight is the same as for the 50 keV electrons in Figure 9. Labels on the curves are arbitrary units.

Figure 11. An estimate of the cutoff latitude as a function of particle energy in the midnight meridian plane.

MAGNETOSPHERIC MODEL

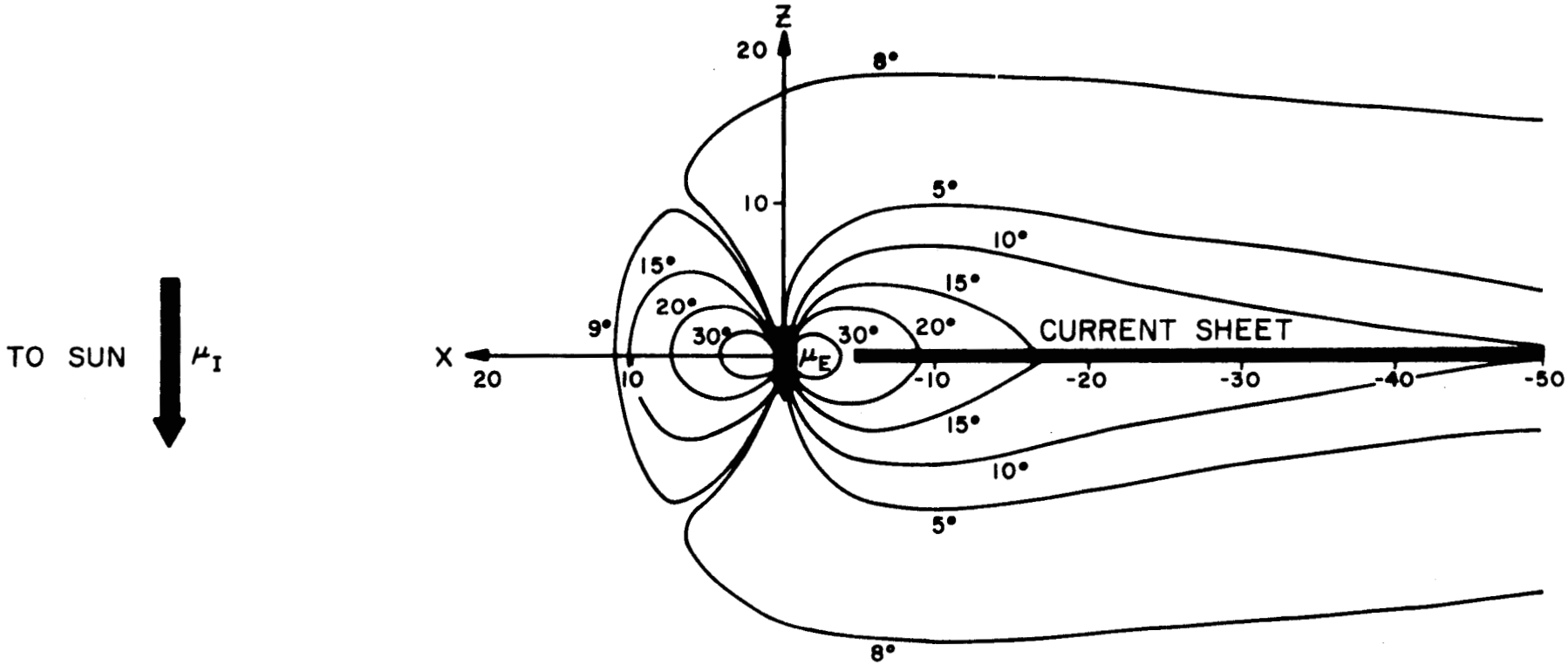

NOON-MIDNIGHT CROSS SECTION

Figure 1

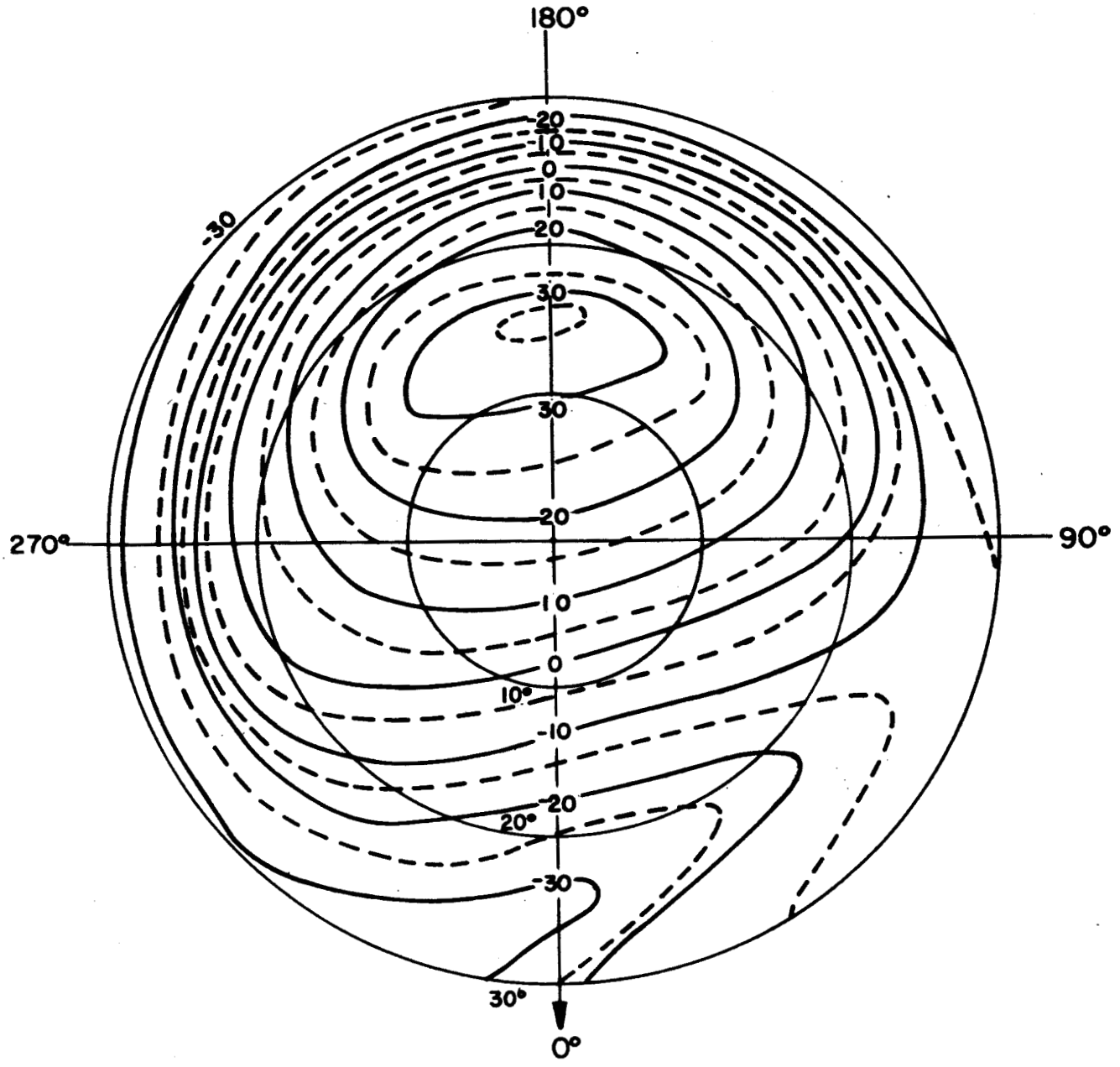

ASSUMED ELECTRIC POTENTIAL SYSTEM

INCLUDES FIELD DUE TO COROTATION

Figure 2

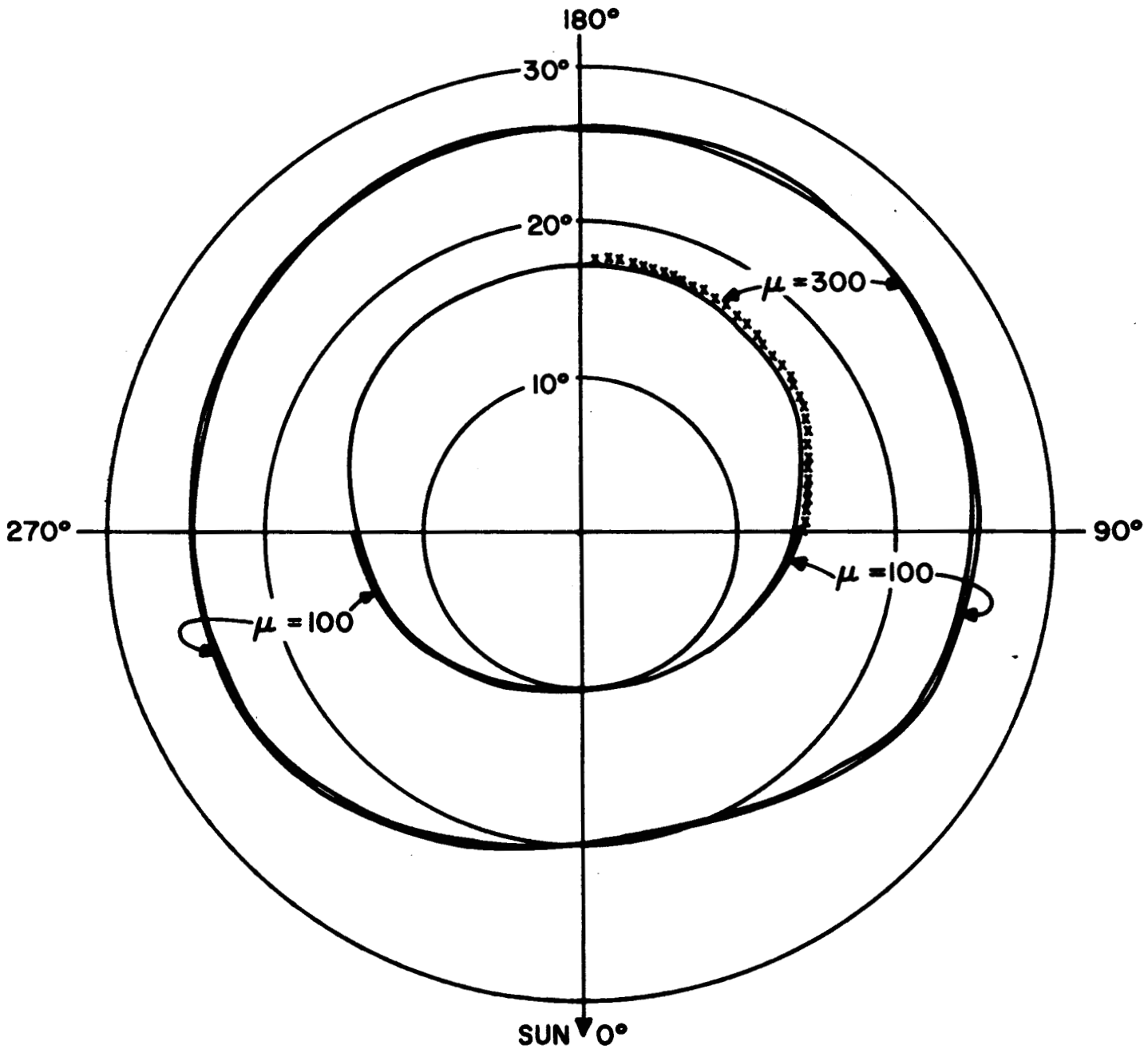

DRIFT PATHS FOR ELECTRONS

K=40 KeV

μ = 100 & 300 KeV/GAUSS

Figure 3

MAXIMUM PATH DIFFERENCES FOR ELECTRONS MEASURED BY INJUN 3 LOW ENERGY DETECTOR

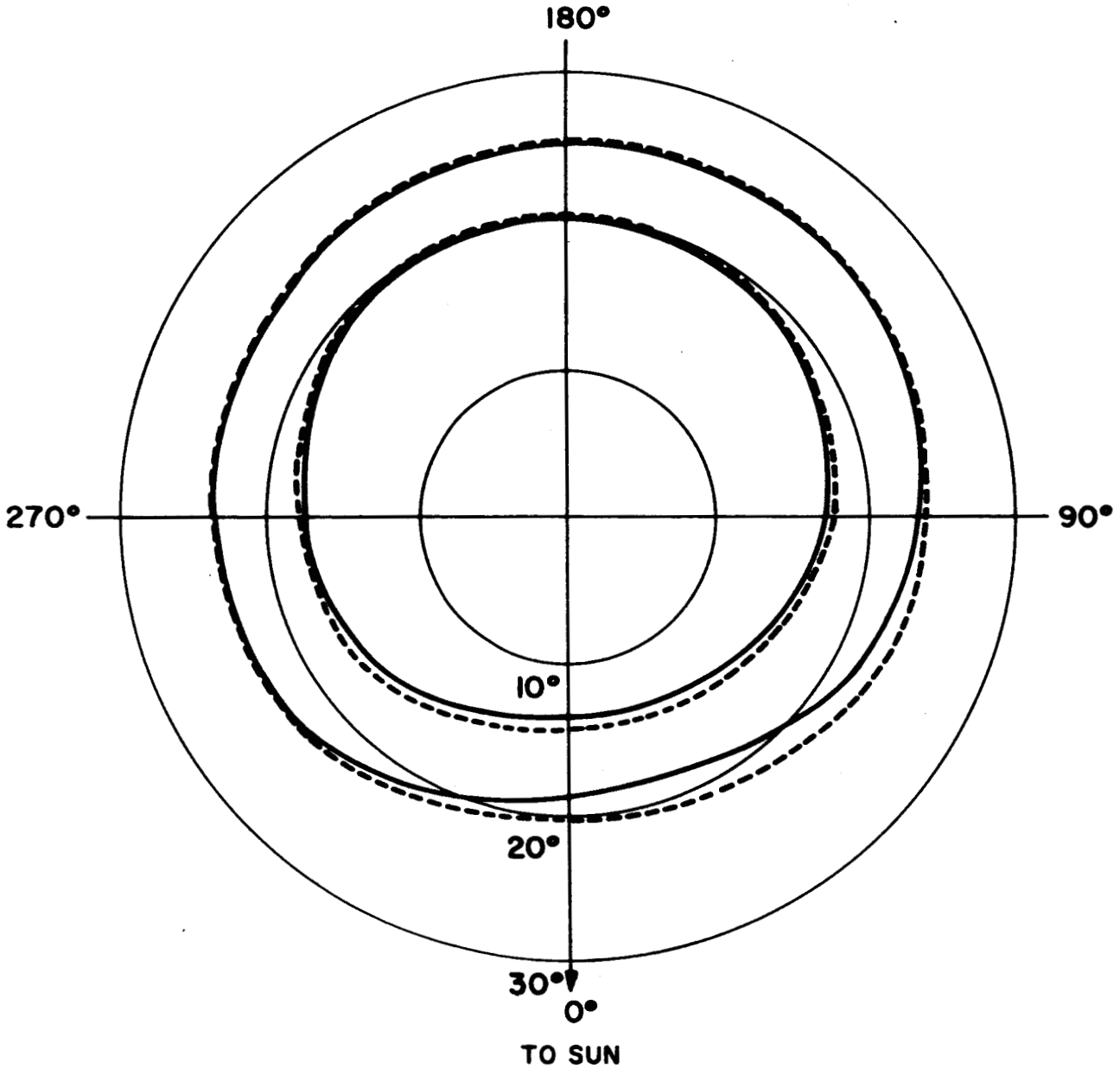

-------- K = 55, μ = 250, μ = 150

——— K = 40, μ = 250, μ = 90

Figure 4

COMPARISON OF CONTOURS OF CONSTANT OMNIDIRECTIONAL INTENSITY OF ELECTRONS ($\alpha = 90 \pm 13°$, $W \gtrsim 40$ KeV) WITH PREDICTIONS OF MODEL

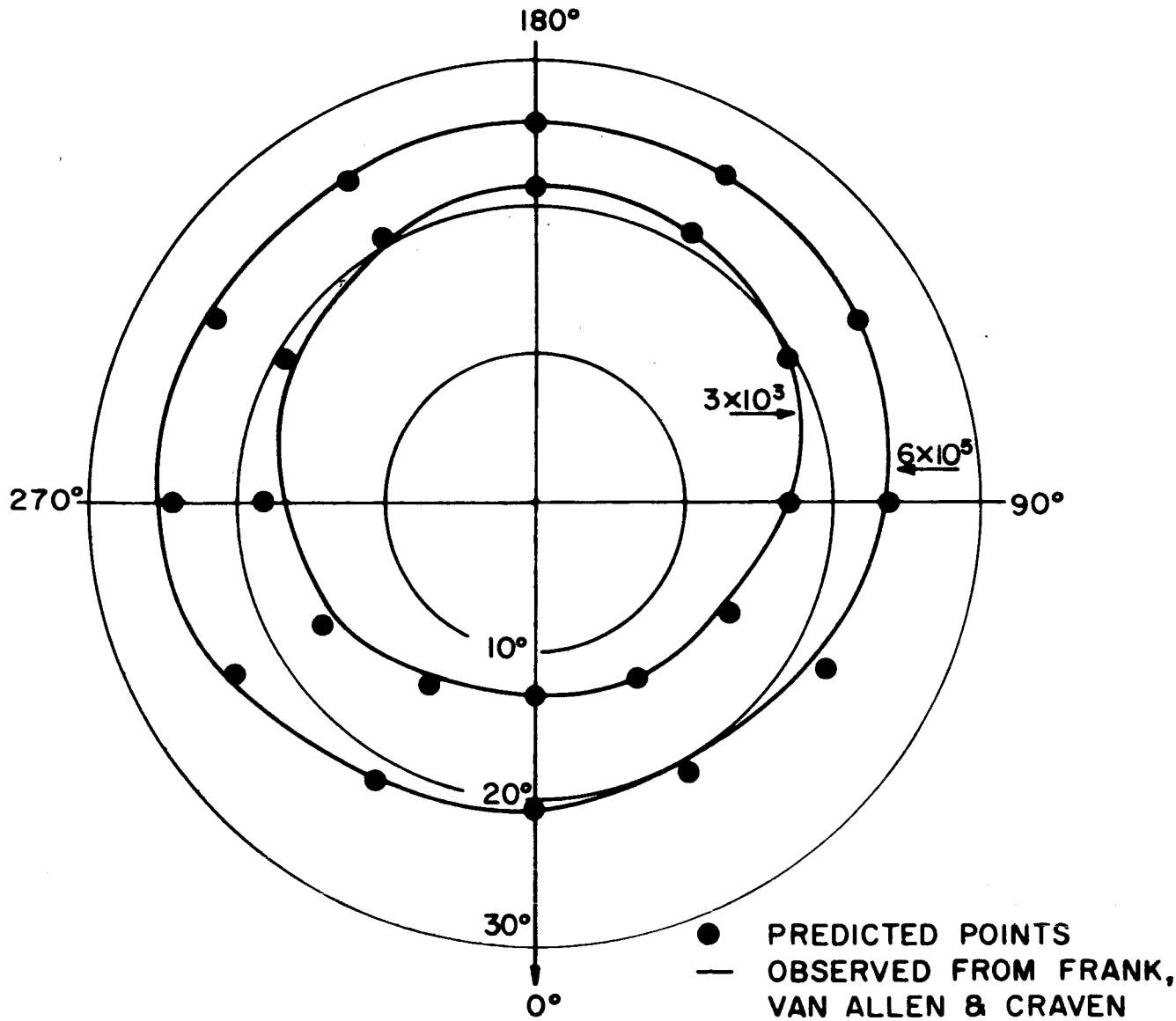

Figure 5

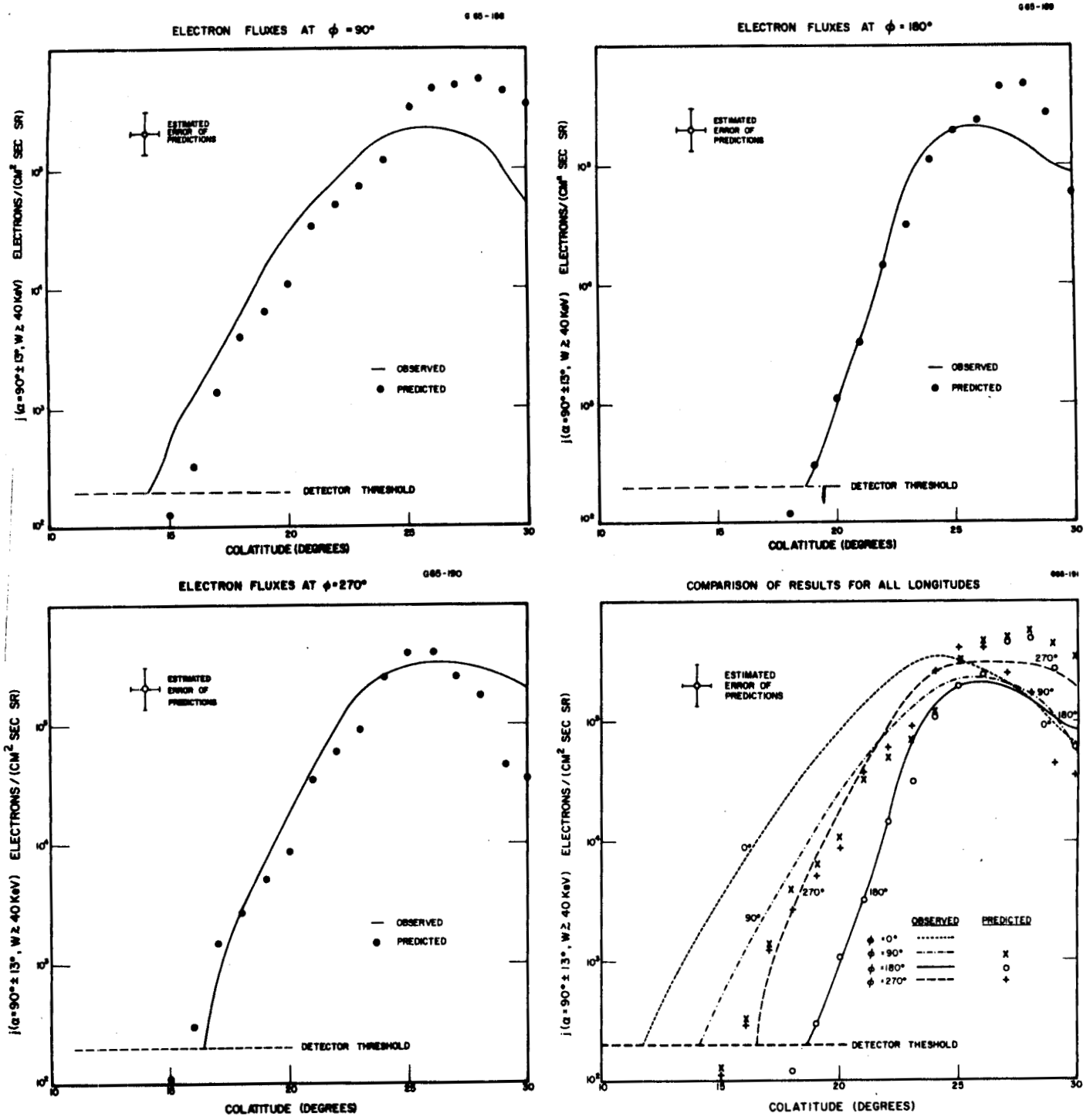
ELECTRON FLUXES AT ϕ = 90°
ESTIMATED ERROR OF PREDICTIONS
OBSERVED
PREDICTED
DETECTOR THRESHOLD
j(α=90°±13°, W≥40 KeV) ELECTRONS/(CM² SEC SR)
COLATITUDE (DEGREES)
ELECTRON FLUXES AT ϕ = 180°
ESTIMATED ERROR OF PREDICTIONS
OBSERVED
PREDICTED
DETECTOR THRESHOLD
j(α=90°±13°, W≥40 KeV) ELECTRONS/(CM² SEC SR)
COLATITUDE (DEGREES)
ELECTRON FLUXES AT ϕ=270°
ESTIMATED ERROR OF PREDICTIONS
OBSERVED
PREDICTED
DETECTOR THRESHOLD
j(α=90°±13°, W≥40 KeV) ELECTRONS/(CM² SEC SR)
COLATITUDE (DEGREES)
COMPARISON OF RESULTS FOR ALL LONGITUDES
ESTIMATED ERROR OF PREDICTIONS
OBSERVED
PREDICTED
ϕ =0°
ϕ =90°
ϕ =180°
ϕ =270°
DETECTOR THESHOLD
j(α=90°±13°, W≥40 KeV) ELECTRONS/(CM² SEC SR)
COLATITUDE (DEGREES)

Figure 6

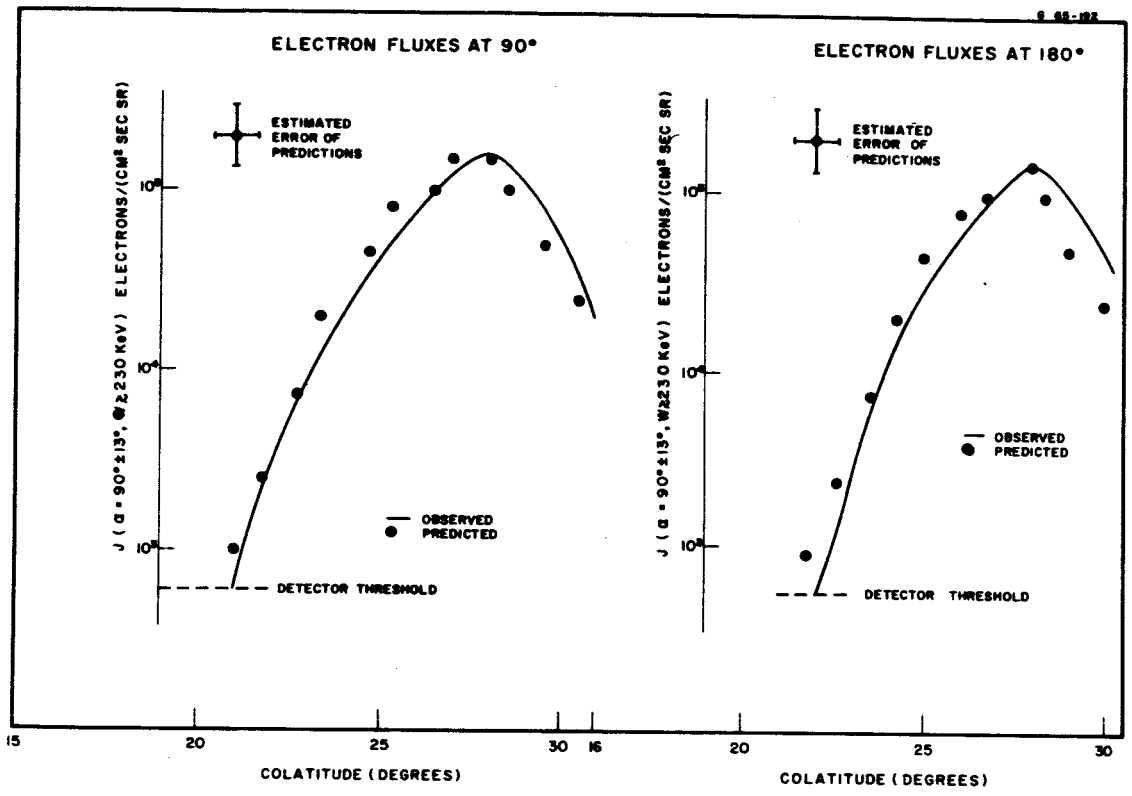
ELECTRON FLUXES AT 90°
ELECTRON FLUXES AT 180°
ESTIMATED ERROR OF PREDICTIONS
OBSERVED
PREDICTED
DETECTOR THRESHOLD
COLATITUDE (DEGREES)

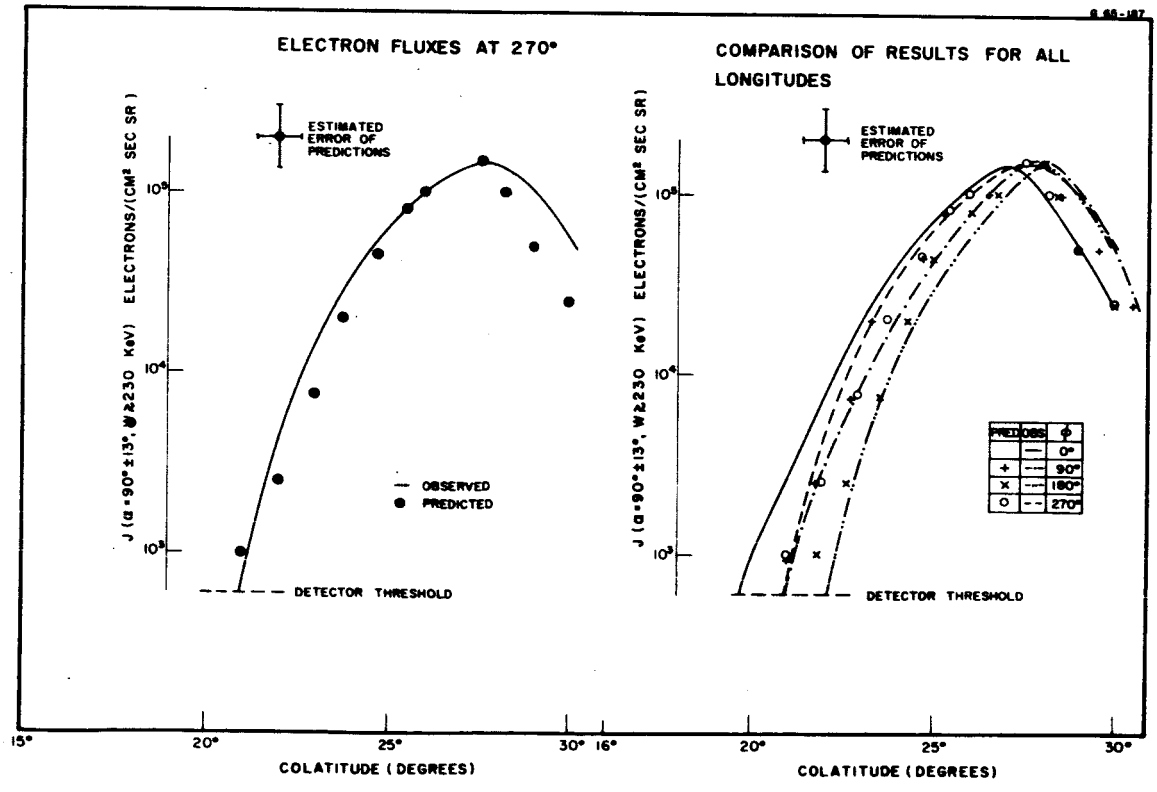
ELECTRON FLUXES AT 270°
COMPARISON OF RESULTS FOR ALL LONGITUDES
ESTIMATED ERROR OF PREDICTIONS
OBSERVED
PREDICTED
DETECTOR THRESHOLD
COLATITUDE (DEGREES)

Figure 7

REGIONS WHERE 10 KeV ELECTRONS MAY BE FOUND MIRRORING AT .3 GAUSS

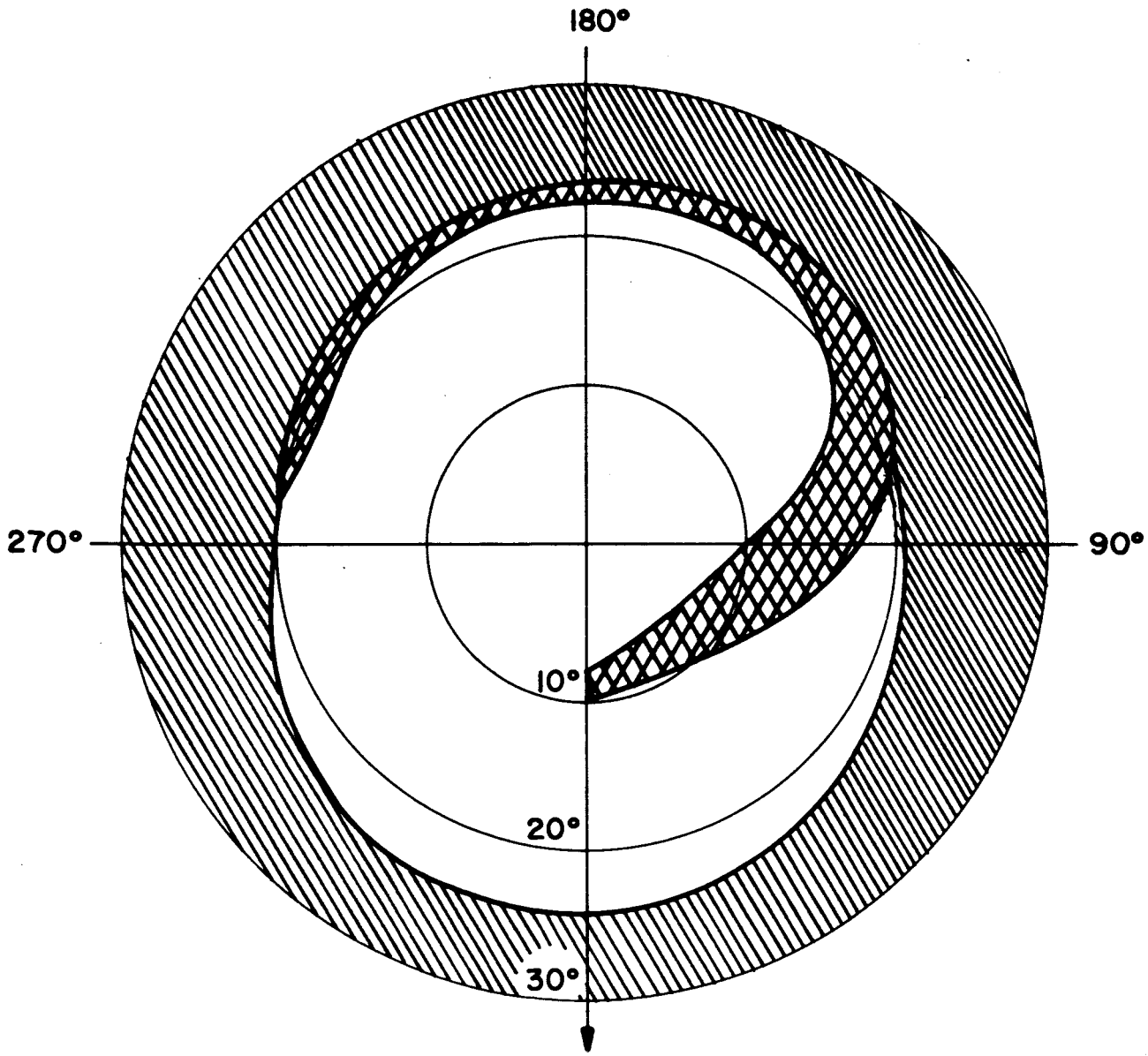

REGION WHERE DURABLY TRAPPED ELECTRONS CAN BE FOUND WITH 10 KeV, MIRRORING AT 0.3 GAUSS

REGION WHERE ELECTRONS ENTERING AT THE NEUTRAL POINT CAN BE FOUND WITH 10 KeV, MIRRORING AT 0.3 GAUSS

Figure 8

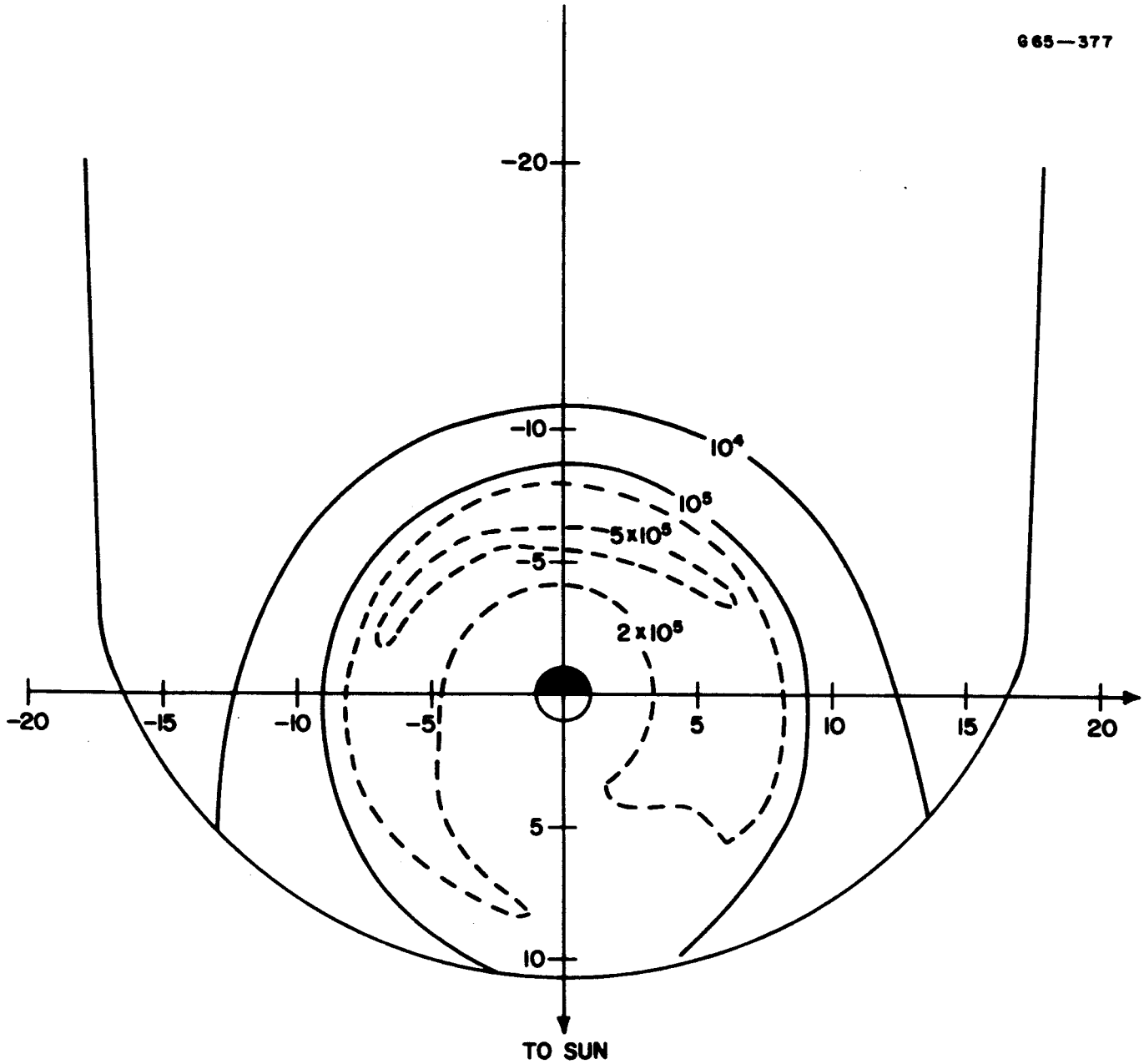

CONTOURS OF CONSTANT DIRECTIONAL INTENSITY OF
50 KeV ELECTRONS IN THE EQUATORIAL PLANE
CONTOURS ARE LABELED WITH $j(W_e = 50\ KeV,\ \alpha \approx 90°)$ IN $\left(\frac{PARTICLES}{Cm^2\ Sec\ Sr}\right)$

Figure 9

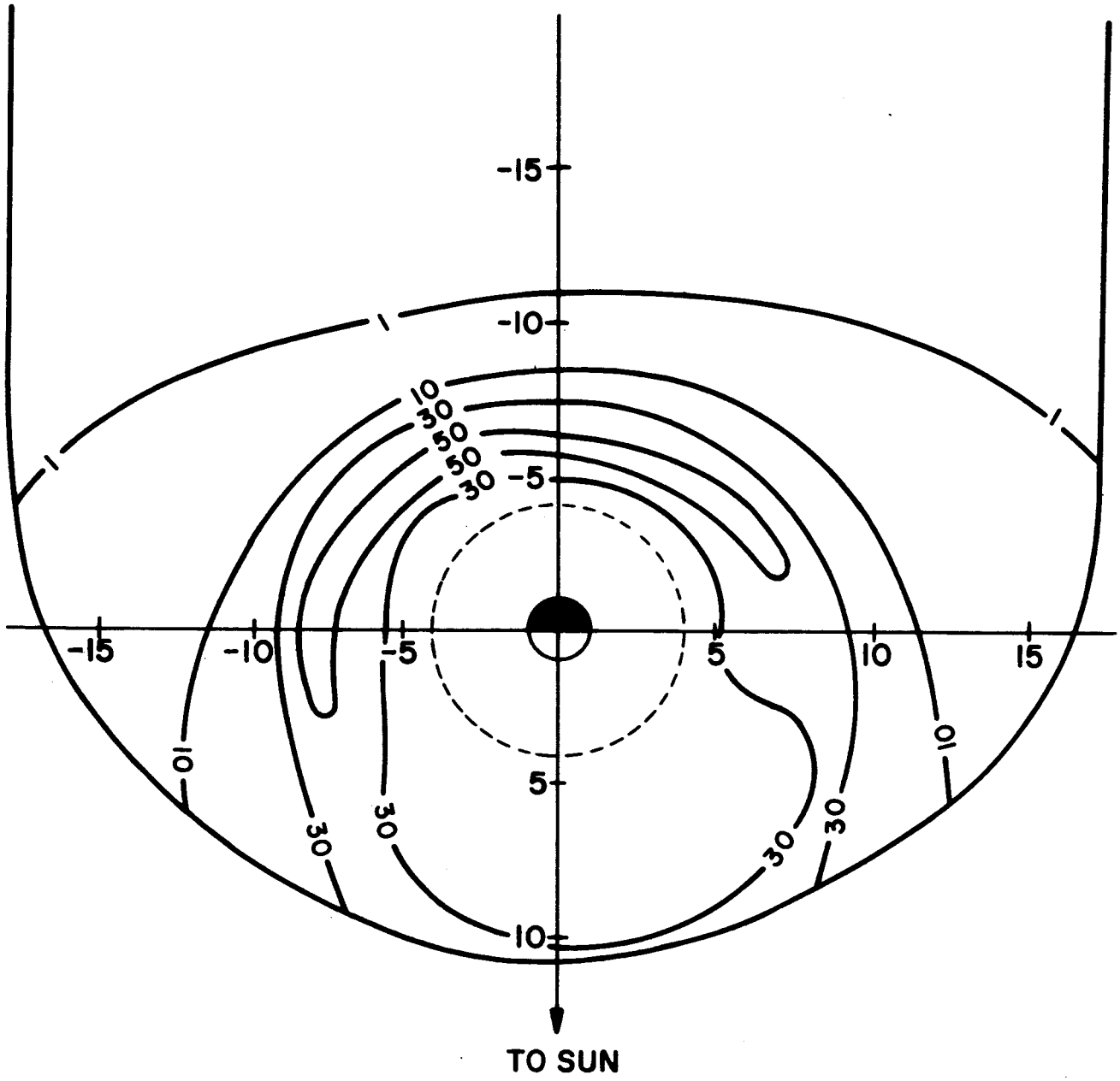

ESTIMATED CONTOURS OF CONSTANT
RELATIVE INTENSITY OF 10 KeV ELECTRONS
IN THE EQUATORIAL PLANE

Figure 10

PARTICLE ENERGY VS MAXIMUM LATITUDE FOR TRAPPING IN THE MIDNIGHT MERIDIAN

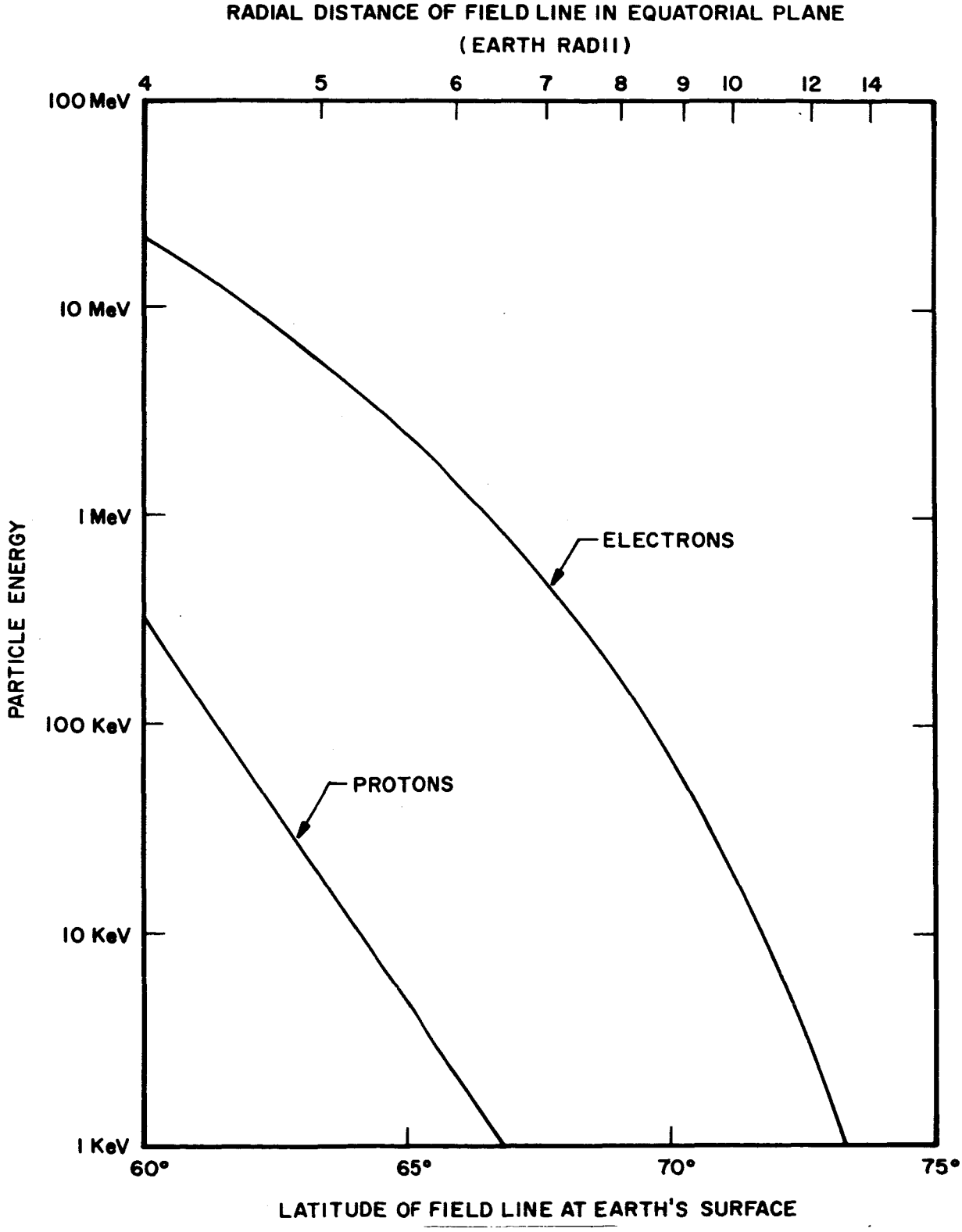

Figure 11